ICES Journal of Marine Science Advance Access published October 19, 2012

ICES Journal of Marine Science

ICES International Council for the Exploration of the Sea
CIEM Conseil International pour l'Exploration de la Mer

ICES Journal of Marine Science; doi:10.1093/icesjms/fss140

A distorted wave Born approximation target strength model for Bering Sea euphausiids

Joy N. Smith[1], Patrick H. Ressler[2], and Joseph D. Warren[1]*

[1]*School of Marine and Atmospheric Sciences, Stony Brook University, 239 Montauk Hwy, Southampton, NY 11968, USA*
[2]*National Marine Fisheries Service, Alaska Fisheries Science Center, Resource Assessment and Conservation Engineering Division, 7600 Sand Point Way NE, Seattle, WA 98115, USA*

**Corresponding Author: tel: +1-631-632-5045; fax: +1-631-632-5070; e-mail: joe.warren@stonybrook.edu*

Smith, J. N., Ressler, P. H., and Warren, J. D. A distorted wave Born approximation target strength model for Bering Sea euphausiids. – ICES Journal of Marine Science, doi.10.1093/icesjms/fss140.

Received 24 May 2012; accepted 3 July 2012.

Acoustic surveys monitor euphausiid populations in the Bering Sea because of their importance as prey for walleye pollock and other organisms. Various scattering models exist to convert acoustic backscatter data to estimates of euphausiid numerical density or biomass, but a target strength (TS) model specific to Bering Sea euphausiids has not been available. This study parameterized a distorted wave Born approximation (DWBA) scattering model using physical (length and body shape) and material (density contrast, *g*, and sound speed contrast, *h*) properties measured from live euphausiids. All model parameters (length, shape, material properties, orientation) were evaluated for their effect on predicted TS. A polynomial function was used to describe animal shape and produced smaller TS estimates compared to a taper function, as is traditionally used in DWBA scattering models of euphausiids. Animal length was positively correlated with TS, but variations in other parameters (including material properties and orientation) also produced large changes in TS. Large differences in TS between estimates calculated using measured versus literature material property values caused large variations in acoustic estimates of euphausiid numerical densities (animals m^{-3}) which emphasizes the importance of collecting site-specific *g* and *h* measurements when possible.

Keywords: distorted wave Born approximation (DWBA), euphausiids, target strength (TS).

Introduction

Euphausiids ("krill", principally *Thysanoessa* spp.) are an important part of the Bering Sea ecosystem. These crustacean zooplankton are prey for many species, including murres (Decker and Hunt, 1996), northern fur seals (Sinclair, 1994), puffins (Hatch and Sanger, 1992), and most notably walleye pollock (*Theragra chalcogramma;* Bailey, 1989; Lang *et al.*, 2000, 2005) as pollock are the target of one of the largest single-species fisheries in the world (FAO, 2009). There are interests in a quantitative estimate of the abundance of euphausiids in the eastern Bering Sea because of the trophic linkage between euphausiids and pollock (Ianelli *et al.*, 2009). Acoustic-trawl resource assessment surveys conducted in the Bering Sea by the National Marine Fisheries Service (Honkalehto *et al.*, 2009) provide a potential source of this information. Acoustic surveys sample large areas at high spatial and temporal resolution (Simmonds and MacLennan, 2005), but net sampling must also be conducted to ground-truth the acoustic data and determine the types of animals being detected (Kasatkina *et al.*, 2004). Once the identity of the dominant acoustic targets are known, a model of the acoustic scattering from these targets is required to convert acoustic backscatter measurements into units of animal abundance and biomass (Foote and Stanton, 2000).

The prevailing approach to modelling the scattering of euphausiids is via physics-based scattering models. These models require input parameters describing the acoustic wave (frequency or wavelength) and the target (shape, length, orientation relative to the acoustic wave, and material properties) (Stanton and Chu, 2000; Lavery *et al.*, 2002; Demer and Conti, 2003a, b; Lawson *et al.* 2006). The material properties used in acoustic modelling are: density contrast (*g*), which is the ratio of the density of the animal to the density of the ambient seawater, and sound speed contrast (*h*), which is the ratio of the speed of sound in the animal to that of the surrounding seawater. Material property

data are often measured through laboratory studies of individual specimens (Greenlaw and Johnson, 1982; Køgeler *et al.*, 1987; Forman and Warren, 2010), although these measurements have also been made at sea (Chu and Wiebe, 2005; Smith *et al.*, 2010). One purpose of this study was to examine the influence of material properties, specifically g and h, on model predictions of Bering Sea euphausiid target strength (TS).

A variety of scattering model formulations have been proposed for euphausiids. Initially, euphausiids were modelled as straight cylinders (Stanton 1988a, b), but more advanced models considered their shape to be deformed (bent) cylinders (Stanton *et al.*, 1993a,b; Stanton and Chu, 2000). Ray-based solutions were used to compute the scattering at different euphausiid orientations; however, ray-based models work best for angles of incidence near normal to the lengthwise axis of the body (Stanton *et al.*, 1993b) and most are only valid at high frequencies where the acoustic wavelength is smaller than the cross-sectional radius of the euphausiid (Urick, 1983). However, Stanton *et al.*, (1993b) presented a ray-based solution with a phase correction that worked at a wider range of frequencies ($ka > 0.3$ where ka is the product of the acoustic wave number, k, and the equivalent cylindrical radius of the animal, a).

More recently, the distorted wave Born approximation (DWBA) model has been used to model the backscatter from euphausiids. The DWBA model is valid for all acoustic frequencies, can be evaluated for all angles of orientation (Chu *et al.*, 1993), and can be applied to arbitrary shapes (Stanton *et al.*, 1998a, b). In the DWBA model, a scattering function is integrated over the length of the axis of the body, taking into account the phase shift that results from the bent body. The model assumes that the targets are comprised of weakly scattering material, which is true for euphausiids. The general formula for modelling acoustic scattering with the DWBA model was first given by Morse and Ingard (1968) as:

$$f_{bs} = \frac{k_1^2}{4\pi} \int_v \int \int \left(\gamma_k - \gamma_\rho\right) e^{i2\left(\vec{k}_i\right)_2 \cdot \vec{r}_{pos}} dv \quad (1)$$

The integration is within the volume (v) of the body and has a position vector ($[r_{pos}]$), $[(\vec{k}_i)_2]$ is the incident wave number vector inside the body, and γ_κ and γ_ρ are terms used to describe the material properties within the body. The parameters γ_κ and γ_ρ are expressed in regards to the compressibility (κ), density contrast (g), and sound speed contrast (h) and are described as follows:

$$\gamma_\kappa \equiv \frac{\kappa_2 - \kappa_1}{\kappa_1} = \frac{1 - g\,h^2}{g\,h^2} \quad (2)$$

$$\gamma_\rho \equiv \frac{\rho_2 - \rho_1}{\rho_2} = \frac{g - 1}{g} \quad (3)$$

where

$$\kappa = \left(\rho c^2\right)^{-1}; h = \frac{c^2}{c_1}; g = \frac{\rho_2}{\rho_1} \quad (4)$$

In this paper, we define the term $|\gamma_\kappa - \gamma_\rho|$ as the material property parameter (M). It will later be parameterized based on g and h measurements for Bering Sea euphausiids.

Since the general formula for the DWBA model is complex and requires knowledge of the animal's shape and material properties in three dimensions, a simplified form of the DWBA model with only one integral has been developed (Stanton *et al.*, 1993a). The single integration assumes that the cross-section of the elongated zooplankton is circular throughout the length of the body and the material properties are constant throughout the animal; therefore the integration follows the length of the body (Stanton *et al.*, 1993a; Stanton *et al.*, 1998b; Stanton and Chu, 2000). It is written as follows:

$$f_{bs} = \frac{k_1}{4} \int_{\vec{r}_{pos}} a\left(\gamma_\kappa - \gamma_\rho\right) e^{2i\left(\vec{k}_i\right)_2 \cdot \vec{r}_{pos}} \frac{J_1\left(2k_2 a \cos\beta_{tilt}\right)}{\cos\beta_{tilt}} |d\vec{r}_{pos}| \quad (5)$$

where a is the radius of the euphausiid as it changes along the length of the animal's body (L), k_1 refers to the acoustic wave number in the surrounding medium, k_2 is the acoustic wave number inside the body, $[(\vec{k}_i)_2]$ is the wave number vector of incident field evaluated inside the body, $ß_{tilt}$ is the angle between the incident wave (k_i) and the cross section of the cylinder at each point along its axis, and J_1 is the Bessel function of the first kind of order one. For modelling purposes, each euphausiid is divided into multiple cross-sectional areas and the energy reflected by each section is calculated separately and added together for the entire animal. The scattering amplitude, f_{bs}, is related to the backscattering cross section of the target (σ_{bs}) and TS by the following relation (Urick, 1983; Medwin and Clay, 1998):

$$TS = 10\log_{10}|f_{bs}|^2 = 10\log_{10}\sigma_{bs} \quad (6)$$

TS is a logarithmic measure of the proportion of the incident intensity backscattered from the target measured in units of dB relative to 1 m^2.

The DWBA model may not properly capture the phases of the backscattered signal for angles away from normal incidence. TS predictions from the DWBA model have been experimentally validated for euphausiids near broadside incidence with angles less than 15–30°; however, the model predictions of TS at larger angles in the same experiment were approximately 5–10 dB lower than direct measurements (McGehee *et al.*, 1998). Demer and Conti (2003a) proposed that the variability in the phases had three possible explanations: scattering variability in a field with stochastic noise, euphausiid shape is more complex than the assumed cylinder with varying radii, and euphausiids flex their body as they swim. They attempted to account for this phase variability using a stochastic distorted wave Born approximation (SDWBA) model validated for Antarctic krill (Demer and Conti 2003a, b). Unfortunately their potential explanations for phase variability in echoes from euphausiids have not been conclusively demonstrated or individually analysed and there is no consensus yet on the best model for euphausiid scattering, though the SDWBA model has been adopted by the Commission for the Conservation of Antarctic Marine Living Resources (CCAMLR) community for krill biomass assessments (Reiss *et al.*, 2008).

In general, the DWBA model has been more widely used than the SDWBA to model backscatter of euphausiids (Lawson *et al.*, 2006; Amakasu and Furusawa, 2006; Lee *et al.*, 2008; Lawson *et al.*, 2008) as well as other animals such as mackerel (Gorska *et al.*, 2005), Japanese anchovy (Miyashita, 2003), salps

(Wiebe *et al.*, 2010), and squid (Jones *et al.*, 2009). Recent studies suggest that euphausiids spend most of their time at orientations where they are nearly horizontal in the water column (Demer and Conti, 2005, Conti and Demer, 2006; Lawson *et al.*, 2006), and for this range of animal orientations there may be little difference between DWBA and SDWBA model predictions. For these reasons we elected to use the DWBA model parameterized using recent measurements of the material properties and shape of Bering Sea euphausiids (Smith *et al.*, 2010) to estimate TS, and evaluate the effects of animal shape, length, material properties, orientation, and curvature on these estimates.

Methods

Animal length, shape, species, and material properties were measured at sea for live euphausiids (Smith *et al.*, 2010) collected in short tows made near the surface at night using a Methot trawl (MT) (Methot, 1986). An MT is a rigid-frame trawl and depressor vane with a 5 m^2 mouth opening, 2 mm × 3 mm oval mesh in the body of the net, and 1 mm mesh in the codend, towed at 2–3 kts. Zooplankton samples were collected at nine stations from 20 June to 9 July 2008 during the Bering Sea acoustic-trawl pollock survey aboard the NOAA Ship *Oscar Dyson* (Figure 1). These data, as well as several different distributions of animal orientation from the literature, were used to parameterize the DWBA model. Since strong species-specific differences in length and material properties were not observed in these data (Smith *et al.*, 2010), euphausiids of all species are modelled using the same parameters. The effect of each model parameter on TS estimates for acoustic frequencies from 10 to 1000 kHz was calculated. MTs conducted on euphausiid layers during daytime were used for comparisons of acoustic and net capture estimates of euphausiid density.

Model parameterization and sensitivity

TS predictions from the single integration DWBA model (Equations 5 and 6) rely on the shape of the euphausiids (L and a), their material properties (γ_κ and γ_ρ), and their orientation and curvature ($ß_{tilt}$).

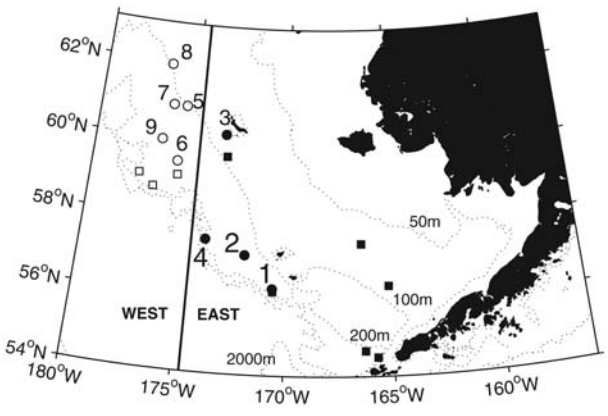

Figure 1. Station locations are shown for Methot trawl (MT) stations (numbered circles) where material property measurements were made, and daytime trawl (DT) stations (squares) where concurrent acoustic and net data were collected. Stations were divided into East (filled) and West (open) regions. DT and MT stations were conducted on different cruise legs during the summer of 2008. Bathymetry contours (dotted lines) are shown for 50, 100, 200, and 2000 m.

Animal Shape

Chu *et al.* (1993) described the shape of the euphausiids using a taper function:

$$a(z) = a_0 * \sqrt{\left[1 - \left(\frac{z}{(L/2)}\right)^T\right]} \tag{7}$$

where T is the taper variable, a_0 is the radius at the midsection of the euphausiid ($z = 0$) which is half of the measured width (widest part of the first thoracic segment), and L is the length of the animal from the anterior tip of its eye stalk to the posterior tip of its telson (Foote, 1990; McGehee *et al.*, 1998; Demer and Conti, 2005). Previous studies of Antarctic krill (Chu *et al.*, 1993; Lawson *et al.* 2006) used a taper value of 10 (taper occurs rapidly near the edge of both ends of the animal), but a taper variable equal to 2 (taper is gradual and begins near the mid-section of the animal) was a better visual match to the shape of the Bering Sea euphausiids. However, a more realistic shape model was created by measuring the animal's height (dorsal to ventral distance), which was later used to calculate the radius, in 0.5 mm increments along the length of the body from digitized images of four Bering Sea euphausiids. The radii were normalized by dividing each radii measurement by the largest radius measurement so that the radius values ranged from 0 to 1. The length of the euphausiid's body was also normalized (to a value of two) and shifted so that the animal's telson was considered to be point −1, the midpoint was 0, and the end of the eye was 1 (Figure 2). This was done to create a length-independent shape function applicable to krill of any size. The normalized radius measurements were then averaged for all animals, and two shape functions (a smoothly-varying sixth-degree polynomial and a segmented five-part piecewise) were fit to these measurements. The new shape function was based on measurements of four animals, but there was little variation between each animal (mean standard deviation in normalized radii was 0.04). The sixth-degree polynomial function, the piecewise function, and the two taper functions (with $T = 10$ and 2), were separately used to describe the shape of the animal in the DWBA model to estimate the TS of euphausiids.

In order to compare the differences in model predictions of TS for the four shapes, the scattering spectra were calculated for each shape function for two different cases, all shapes with the same mean radii (1.5 mm) and different volumes ($T = 10, v = 5.98$ mm^3; $T = 2$, $v = 5.03$ mm^3; polynomial $v = 2.34$ mm^3, and piecewise $v = 1.68$ mm^3), and all shapes with the same volume (5.98 mm^3) but different radii ($T = 10$, $r = 1.0$ mm; $T = 2$, $r = 1.1$ mm; polynomial $r = 1.6$ mm, and piecewise $r = 0.9$ mm). In general, TS models are parameterized using length and width (or height) measurements (not using animal volume); however, varying volumes can have an effect on TS as well as the frequency response of the scattering. Thus, both scenarios (constant radii and varying volumes, varying radii and constant volumes) were examined and calculations were made over the frequency range of 10–1000 kHz.

Animal length

TS was estimated for each euphausiid measured in this study using the measured values in animal length, g, and h, and the DWBA model. Assuming the orientation of a euphausiid does not change, the TS will increase with the length of the animal, although

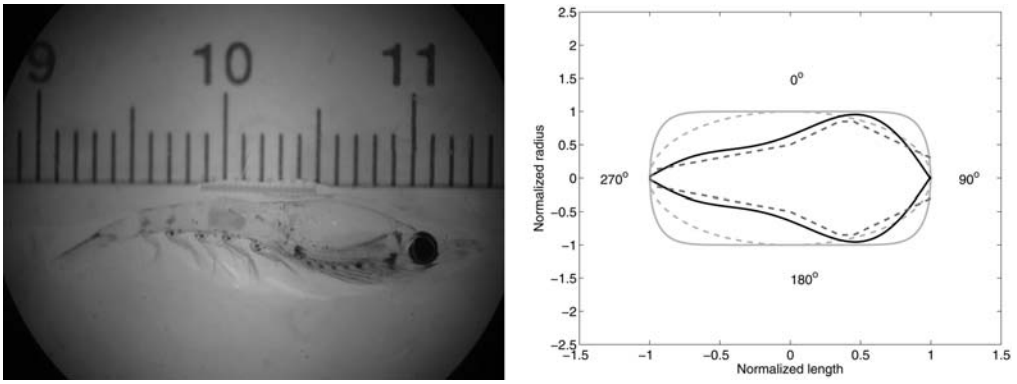

Figure 2. An image of a euphausiid (left, scale is cm) and the different functions (right) used to define the euphausiid shape in the TS model: taper (T) = 10 (solid grey), T = 2 (dashed grey), polynomial (solid black), and piecewise (dashed dark grey). The incidence angle is also included where 0° is broadside incidence. Notice that the polynomial and piecewise functions more accurately represent the shape of the euphausiid.

this relationship is not linear (Chu et al., 2000). By applying the measured g and h values to the DWBA model, the range of TS values for different length measurements was examined at a frequency of 120 kHz.

Material properties

Measurements of material properties of live Bering Sea euphausiids (Smith *et al.*, 2010) were used to parameterize the TS model. In that study, g was measured for individual euphausiids, whereas h measurements were made on multiple groups of euphausiids from the same MT. These measurements were averaged together and the mean h value was assigned to each individual euphausiid in that MT. We also examined whether g and h measured at the same location were correlated.

The effects of g and h on TS model predictions were examined by calculating TS values using the minimum, maximum, and mean g and h values observed in the Bering Sea, as well as selected g and h values from other studies (Greenlaw and Johnson, 1982; Køgeler *et al.*, 1987; Chu and Wiebe, 2005) for an animal with mean length and broadside incidence at a frequency of 120 kHz, while the other parameters (orientation, shape, length) were kept constant. The material property value (M) was calculated for each individual animal using measured values of g and h and then averaged for each MT to produce a site-specific M value. This value was used to calculate the mean TS for euphausiids at each location.

Animal orientation and curvature

Animal orientation (θ) is the angle between the line joining the bent cylinder's ends and the horizontal plane (Lawson *et al.*, 2006). In order to determine the influence of orientation on TS estimates, several different Gaussian distributions describing animal orientation were applied to the DWBA model. The distribution of orientations observed for euphausiids measured in an aquarium was found to be $N(\theta,\sigma_\theta) = N(45.3,30.4)$ by Kils (1981) and $N(\theta, \sigma_\theta) = N(45.6,19.6)$ by Endo (1993), where θ is the mean angle of orientation and σ_θ is the associated standard deviation. *In situ* observations of euphausiid orientation include N(9.7,59.3), N(0,27.3) (Lawson *et al.*, 2006), and N(0,30) (Kristensen and Dalen, 1986). Distributions of *in situ* euphausiid orientation estimated by inversion of euphausiid scattering models include N(15,5) (Demer and Conti, 2005) and N(11,4) (Conti and Demer, 2006).

Both the animal's orientation and the radius of curvature (ρ_c) are used to define the parameter $ß_{tilt}$. Assuming the echosounder is pointing down through the water column, an animal is at normal (broadside) incidence ($\theta = 0°$) if it is horizontal in the water column. At the midpoint of the euphausiid, $ß_{tilt} = \theta$, however this relationship does not hold true along the length of the euphausiid because of the curvature of its body. The mean radius of curvature was determined for the euphausiids examined in this study (using the geometry described in Stanton, 1989). Assuming that ρ_c remains constant for all euphausiids, a single value of ρ_c was applied.

Estimates of euphausiid numerical density

A Simrad EK 60 echosounder and vessel-mounted acoustic transducers located on a lowered centerboard 9.15 m below the sea surface were calibrated via the standard target method (Foote *et al.*, 1987) and used to measure volume backscattering strength (S_v, dB re 1 m^{-1}) at five frequencies (18, 38, 70, 120, 200 kHz). S_v is the logarithmic measure of combined echo intensity from multiple scatterers in a given volume, which can be used to estimate the numerical abundance of scatterers. The linear form of S_v is the volume backscattering coefficient (s_v, m^{-1}) (Simmonds and MacLennan, 2005).

Concurrent comparisons of s_v and the density of euphausiids estimated from night-time Methot tows used to capture live specimens for g and h measurements were not possible. These night-time tows collected euphausiids in the upper 10–20 m of the water column where s_v data were not available because of the depth of the vessel-mounted transducers and the necessary blanking distance beneath the transducers to account for pulse transmission and transducer ringing. Instead, nine day-time Methot tows that were deployed to sample length and species composition of euphausiid scattering layers located well below the sea surface (identified based on their frequency response; De Robertis *et al.*, 2010; Ressler *et al.*, 2012) were used to compare acoustic and net tow estimates of euphausiid numerical density. Smith *et al.*, (2010) found spatial variation in euphausiid material properties between the east and west sides of the study site, so the nine day-time tows (DTs) were grouped accordingly, with DT 1–6

constituting the East region and DT 7–9 comprising the West region (Figure 1). Values of M were determined for each DT (based on the region) and the length distribution data gathered from each DT were used to estimate a length-weighted σ_{bs} for each DT using the DWBA model. The mean sv over the portion of the water column sampled by each day-time MT was calculated, accounting for the mouth area of the net, the amount of wire out during the net deployment, and the setback between acoustic transducers and the net frame. Observed sv and σ_{bs} were used to calculate the number of animals (n) present in one m^3 of water using the equation:

$$s_v = \sum_{i=1}^{m} N_i \sigma_{bs_i} \tag{8}$$

where m is the number of different types of scatterers in the volume. It was assumed that euphausiids were the dominant acoustic target ($m = 1$). This acoustically-estimated quantity was compared with numerical density estimated from the flowmeter-equipped MT. This procedure was followed for all nine DTs.

Results

TS values for individual euphausiids were calculated for all MTs and scattering model input parameters were varied to determine their effect on euphausiid TS. In order to evaluate the influence of one parameter on TS estimates, other parameters were kept constant and the mean material properties and animal length were used (Table 1; Smith *et al.*, 2010).

Animal shape

From measurements of radius along the length of the body, an average euphausiid shape was defined by fitting a sixth-degree polynomial to the data:

$$a = 0.83z^6 + 0.36z^5 - 2.1z^4 - 1.2z^3 + 0.63z^2 + 0.82z + 0.64 \tag{9}$$

where z is the normalized length of the animal ranging from −1 to 1 and a is the animal radius in mm. The same data are also described by the following piecewise function:

$$\begin{array}{ll} z = -1 \text{ to } -0.95 & a = 2.5z + 2.5 \\ z = -0.95 \text{ to } 0 & a = 0.39z + 0.5 \\ z = 0 \text{ to } 0.35 & a = z + 0.5 \\ z = 0.35 \text{ to } 0.45 & a = 0.85 \\ z = 0.45 \text{ to } 1 & a = -1z + 1.3 \end{array} \tag{10}$$

The polynomial shape function is smoothly-varying along the animal length and resembles the actual animal shape more closely. In contrast, the piecewise function has sharp changes in the shape of the animal along the body length. The taper function (using both taper variables $T = 10$ and 2) assumed that the euphausiid was symmetrical (dorsal-ventral) while the polynomial and piecewise functions do not (Figure 2).

When the radius was kept constant but the volume changed for each shape equation, the polynomial and piecewise functions had smaller TS values compared to the taper functions for most frequencies, although this varied with some frequencies depending on the behavior of the function (Figure 3). There was a considerable difference in TS values between the functions; for example, at

Table 1. Minimum, maximum, and mean of physical and material properties measured for Bering Sea euphausiids ($n = 380$).

	Min	Max	Mean
Length (mm)	12	27	18.2
Height (mm)	1	5	2.5
g	1.001	1.041	1.017
h	0.9898	1.014	1.005

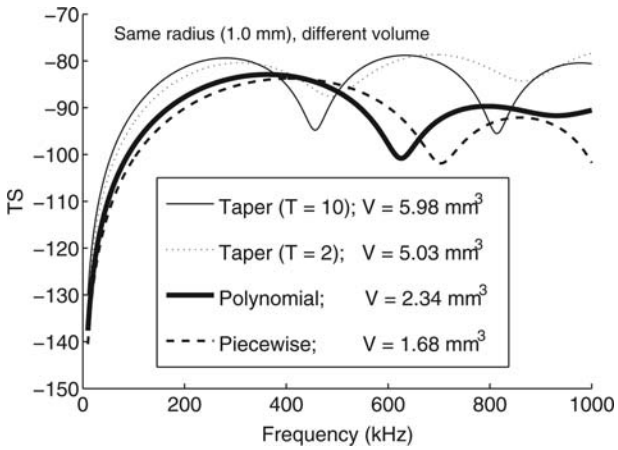

Figure 3. TS (dB re 1 m^2) calculated as a function of frequency for individual Bering Sea euphausiids with measured mean length (L), density contrast (g), and sound speed contrast (h) values. Calculations were made for an animal with broadside incidence and polynomial shape. Constant radius ($r = 1$ mm) was used for each euphausiid shape, while the volume (V) varied among shape models.

120 kHz TS estimates were 7 dB higher than those obtained using the polynomial shape function, and nearly 10 dB higher than those using the piecewise shape function. The resulting higher TS values are not unexpected considering the animal volume is larger for both taper functions than for the more realistic polynomial or piecewise shapes (Figure 2). To compare differently-shaped animals with an equivalent volume, TS was also calculated as a function of frequency for animals with the same volume of 5.98 mm^3 (not shown). To maintain the same volume, the radius for each shape function was different ($T = 10$, $r = 1$ mm; $T = 2$, $r = 1.1$ mm; polynomial $r = 1.6$ mm; piecewise $r = 1.89$ mm). As was true for the same radius but different volumes scenario, in nearly all cases where the volume was constant but the radius changed, the polynomial and piecewise functions had smaller TS values compared to those obtained using the taper function for most frequencies. In both cases, the use of differently-shaped models also changed the shape of the TS curve as a function of frequency, altering the location of peaks and nulls (Figure 3). Since the polynomial shape model most closely matched the shape of the euphausiids we examined, it was used in subsequent scattering model calculations.

Animal length

As expected when TS was calculated for different lengths using the g and h measurements for each individual euphausiid, TS increased with animal length (Figure 4). There was, however, a wide range in TS for each length measurement, with some lengths having nearly a 30 dB difference. This range in TS values

for one length measurement indicates that a significant portion of variability in TS comes from the other parameters.

Material properties

TS was evaluated as a function of frequency for the most common echosounder frequencies used in fishery surveys (18, 38, 70, 120, and 200 kHz) over a range of g and h values including the minimum, mean, and maximum values from measurements of individual Bering Sea euphausiids, as well as measurements of euphausiids in other studies. Each calculation of TS was made with either g or h varying while other model parameters were held constant at the mean values observed for Bering Sea specimens (Table 1) and at broadside incidence using the polynomial shape function. As both material properties increased, so did the TS estimates, although not linearly (Figure 5; these calculations were made at 120 kHz, but the relationship holds true for all frequencies in the geometric scattering regime). Linear regression was used to test for a relationship between the two material properties, but there was no significant correlation between mean g and h for Bering Sea euphausiids at each MT station where both properties were measured ($r = -0.22$, $p = 0.59$, $n = 8$; Figure 6). However, the relationship between g and h is difficult to evaluate, because g is measured on individual animals, and h is measured on groups of animals.

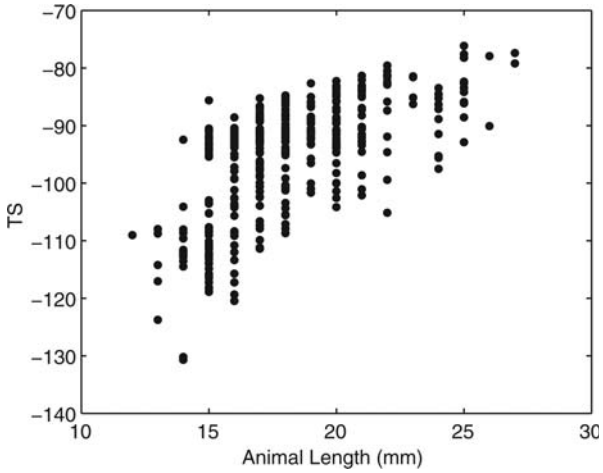

Figure 4. TS (dB re 1 m^2) calculated for each individual euphausiid collected from the Bering Sea ($n = 380$) using the measured L, width, g, and h, the polynomial shape function, a frequency of 120 kHz, and a broadside orientation.

Since there is not a simple relationship between g and h, the minimum g and h values do not necessarily produce the minimum TS value; likewise, the maximum g and h values do not necessarily produce the maximum TS value, and the mean material properties of Bering Sea euphausiids may not be correctly represented by the mean (g) and mean (h). To determine average TS values, mean TS was calculated for each MT using the mean M (material property parameter, a function of both g and h) instead of mean g and h (Table 2).

The large variability in g and h measurements emphasizes the importance of measuring material properties at each new study site, since differences in g and h measurements can have large effects on TS estimates (Chu *et al.*, 2000). Often literature values of g and h (from other geographic locations or even different species) are used in TS models, however this approach (while practical) can produce substantially different TS estimates compared with a site-specific approach (Table 3).

Animal orientation and curvature

The mean radius of curvature for the euphausiids examined was $\rho c = 3.3L$. Stanton *et al.* (1993a) estimated euphausiid curvature to be $3L$, although they also showed that when backscattering cross-sections are averaged over a range of angles then they are nearly independent of ρc when $\rho c \geq 2L$ (which is true in this study). A linear regression found no significant difference in the

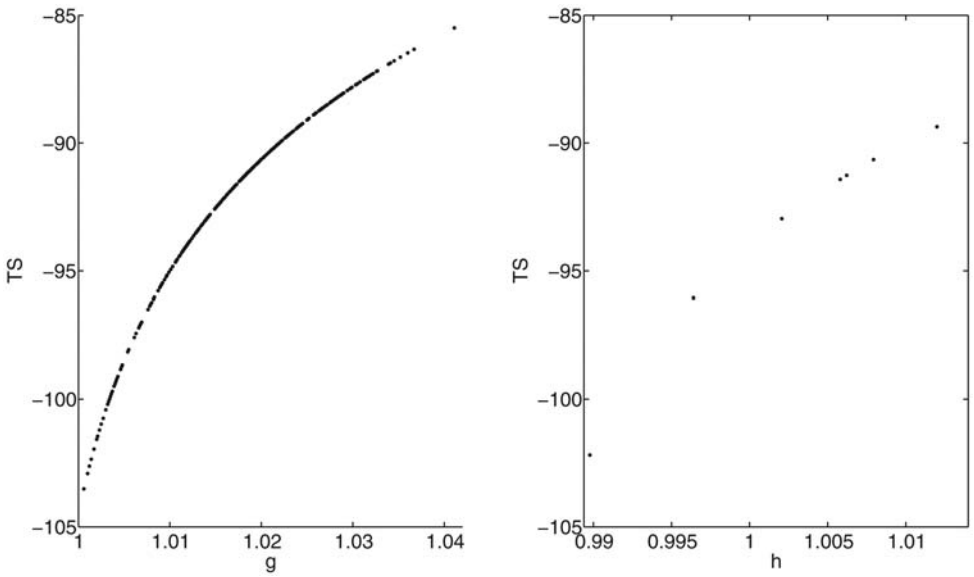

Figure 5. TS (dB re 1 m^2) estimates as a function of g (left panel, other parameters: mean L, mean h, 120 kHz, broadside incidence, polynomial shape) and as a function of h (right panel, other parameters: mean L, mean g, 120 kHz. broadside incidence, polynomial shape). Measurements of h were made on groups of animals, so there are fewer observations than for the g measurements.

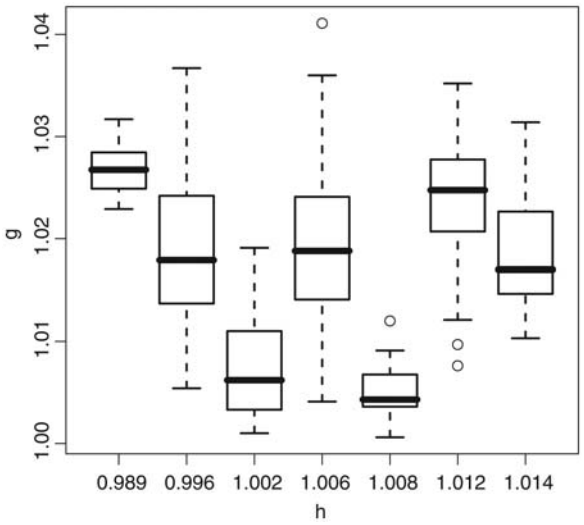

Figure 6. Boxplot of density contrast (g) as a function of sound-speed contrast (h). Boxplots indicate 25th, 50th, and 75th percentiles, whiskers indicate the 95% confidence interval, and outliers are shown as circles. Note that g is measured on individuals while h is measured on groups of animals. No correlation between the two properties is indicated.

Table 2. The mean material property parameter (M) and associated standard deviations calculated for each MT and the resultant mean target strength (TS).

	M		
MT	**mean**	**s.d.**	**TS**
1	0.026	0.005	−98.6
2	0.018	0.009	−101.5
3	0.032	0.022	−96.8
4	0.045	0.009	−93.7
5	0.070	0.010	−89.9
7	0.032	0.005	−96.7
8	0.067	0.016	−90.3
9	0.057	0.011	−91.7

M was not calculated for MT06 because there was no h value collected for that location. Calculations were made using the M value and mean length from each MT at 120 kHz and broadside incidence.

Table 3. Target strength (TS) values were calculated by maintaining mean parameters and altering either g or h separately.

g	h	ΔTS
g_{min}	h_{min}	−7.3
	h_{mean}	−11.2
g_{mean}	h_{min}	−1.8
	h_{max}	+2.9
	h_{Foote}	+6.0
	$h_{Køgeler}$	+6.6
	$h_{Chu\ and\ Wiebe}$	+9.1
g_{max}	h_{mean}	+6.2
	h_{max}	+7.7
$g_{Greenlaw\ and\ Johnson}$	h_{mean}	+7.7
$g_{Køgeler}$	h_{mean}	+9.3

This table gives the difference in TS values away from the TS estimate using mean parameters (i.e. difference in TS away from g_{mean} or h_{mean}). Material properties used from other studies are as follows: $g_{Greenlaw\ and\ Johnson}$=1.050, $g_{Kogeler}$ = 1.062, h_{Foote} =1.0279, $h_{Kogeler}$ =1.031, and $h_{Chu\ and\ Wiebe}$ = 1.048. Mean length was used in calculations for an animal at broadside incidence with a polynomial shape.

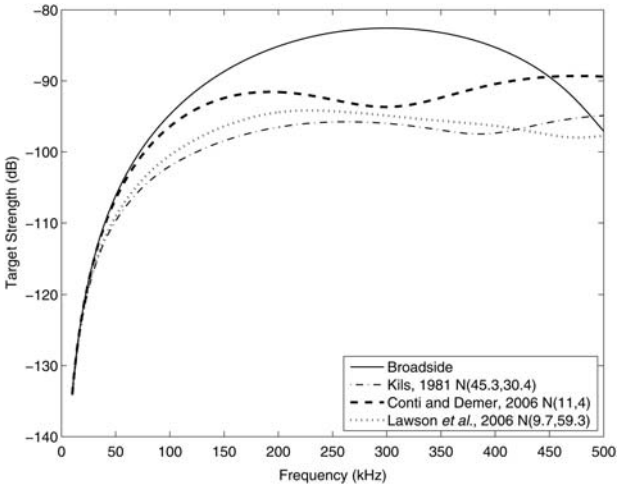

Figure 7. Modelled euphausiid TS as a function of frequency for several different orientation distributions N(mean, standard deviation): N(0,0) broadside incidence, N(45.3,30.4) from Kils (1981), N(11,4) from Conti and Demer (2006), and N(9.7,59.3) from Lawson *et al.* (2006). The mean length and material properties were used to calculate the TS for a polynomial shaped euphausiid.

TS estimate when using either $\rho c = 3.3L$ or $\rho c = 3L$; thus, $3.3L$ was used for all subsequent computations.

Across a range of frequencies, orientation had a large impact on TS estimates made using various distributions of euphausiid orientation reported by other studies (Figure 7). Polynomial shape, mean length, and mean material properties were used to compute TS at each combination of orientation and frequency. Broadside incidence (i.e. dorsal insonification) produced the largest TS values and the least amount of peaks and nulls across the range of frequencies. As expected, orientation distributions near broadside incidence (N(15,5) from Demer and Conti, 2005, and N(11,4) from Conti and Demer, 2006) produced TS estimates similar to those produced when the animal was oriented at broadside incidence. The euphausiids described by Kils' (1981) orientation distribution are not horizontal in the water column and are at an angle (45.3°) with a large standard deviation (30.4); consequently, this orientation distribution produced the lowest TS estimates.

Estimates of numerical density at these tow locations

Numerical densities were calculated for nine DT locations using observed Sv, measured euphausiid lengths, and either the mean M for the study or the East or West region containing the tow. DWBA model calculations were made at 120 kHz for euphausiids at broadside incidence with a polynomial shape. When the numerical densities derived from acoustic data were compared to those estimated from the net tow catches, the acoustic estimates were always larger, often by several orders of magnitude (Figure 8). Site-specific information on material properties in TS model computations changed acoustic estimates of euphausiid density in scattering layers by a factor of 0.6–2.1 across these locations, and

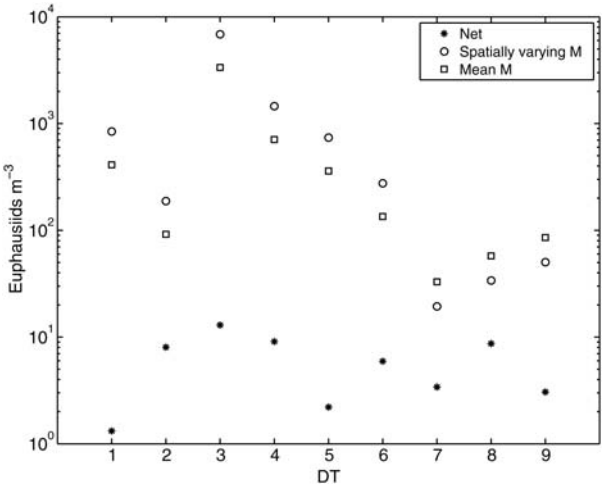

Figure 8. Comparison of numerical densities at nine daytime trawl (DT) stations from net measurements and two acoustic methods which used measured Sv data, euphausiid length data from the DT net tows, and material property measurements from nearby MT stations. Sv data were inverted for euphausiid numerical densities by calculating a length-weighted, mean target strength (TS) value for each DT location. Material property (*g*, *h*) values in the model were either the mean M value for all data collected or were averages for the East and West regions of the study area (see Smith *et al.*, 2010 for reasons for the differences). TS calculations were made for backscatter at 120 kHz for polynomial-shaped euphausiids at broadside incidence. Note that numerical densities are presented on a logarithmic scale.

increased the overall mean numerical density by a factor of 2 when compared to acoustic estimates which used a single mean M value for the entire region. Averaging over all sites in the study, euphausiid numerical densities (# m^{-3}) were 6 (net), 1200 (acoustic using site-specific M values), and 600 (mean M value).

The potential importance of using site-specific animal information for TS can be further demonstrated by a closer examination of the DT numerical density data. Station pairs were selected that had equivalent acoustically-estimated numerical densities using either the site-specific or mean M values. Only one pair (DT 2 and 9) met this criterion where the acoustic estimates of numerical density (using a mean M value) were equivalent (92 and 86 animals m^{-3} respectively). Using single values for animal material properties is the standard procedure in acoustic surveys, so these data reflect what most acoustic surveys of euphausiid abundance would produce and suggest that the animal abundance at these two sites was similar. However, net tow numerical density data showed the numerical densities at DT 2 to be approximately three times greater than at DT 9 (8 and 3 animals m^{-3} respectively). This pattern was also seen when site-specific M values were used to acoustically estimate numerical densities, with DT 2 being 3.5 times as dense as DT 9 (188 and 50 animals m^{-3} respectively). Given that only one pair of sites could be compared in this manner, these results are not conclusive.

Discussion

A DWBA model was parameterized using observed physical and material properties from live Bering Sea euphausiid specimens. Examination of model results indicated that the more realistic empirical model of euphausiid shape and locally-measured, spatially-varying material properties could have a significant effect on model predictions of TS and resulting estimates of numerical density. Parameterization of the expected distribution of euphausiid orientations *in situ* also had a strong influence on model results.

Effect of shape

The sixth degree polynomial model presented in this study most realistically portrays the animal as being asymmetrical from head to tail. Unlike the piecewise function, it does not contain inflection points or abrupt changes in the animal width. The taper function produced higher TS estimates than polynomial and piecewise functions for animals of the same length but different volumes, as well as for animals of the same volume but different lengths, furthermore suggesting that the chosen shape function is important to model predictions. TS estimates for Bering Sea euphausiids in this study produced using the more realistic polynomial model of animal shape will be lower (and lead to higher acoustic estimates of euphausiid density) than those produced with models that use a taper function.

Effect of length

There was a clear, positive relationship between animal length and their model-estimated TS (Figure 4), varying by approximately 30 dB over the lengths observed in this study. Length and width measurements are critical to more accurately parameterizing scattering models in acoustic surveys, and these measurements are relatively easy to collect with standard net or optical zooplankton sampling techniques.

Effect of material properties

Material properties were highly influential on model predictions. Both *g* and *h* were shown to increase TS as *g* or *h* diverged from unity, with TS varying by 15–20 dB, although this relationship was not linear (Figure 5) as was found by Chu *et al.*, 2000. Density contrast (*g*) had a greater influence on the TS estimate compared to sound speed contrast (*h*),although this may be the result of the measured *g* being more variable than measured *h*. The range of TS calculated using the highest and lowest M values measured in the Bering Sea was smaller than the range of TS calculated from material properties measured in this study and values reported in the literature (Table 3), demonstrating that taxon- and area- specific measurements of material properties help reduce and characterize uncertainty in model predictions.

Even with site-specific measurements of *g* and *h*, there are uncertainties associated with the measurement methods (in particular the time-of-flight method) that may produce error (or uncertainty) in the modelled TS (Smith *et al.*, 2010). Our estimates of the TS of Bering Sea euphausiids are generally lower than what would have been calculated had we assumed material property values for other euphausiid species from other locations, as is typically done in acoustic surveys. Since *g* and *h* measurements showed large variability, and the way in which these physical quantities vary together in individual animals is unclear, we contend that mean M (a function of both *g* and *h*) should be used in scattering model predictions instead of mean *g* and mean *h*.

Material properties which are difficult to measure have been shown to be related to a variety of different factors including animal size, water temperature, density, sound speed, or chlorophyll-a concentration, often simpler to measure (Smith *et al.*, 2010). In the future, it may be possible to predict values

of material properties from these more easily-measured parameters but this requires a better understanding of how and why *g* and *h* vary in animals. Until we have more knowledge on this subject, measuring *g* and *h* directly is the best way to have the most accurate TS estimates for a particular acoustic scatterer.

Effect of orientation

We were not able to measure the *in situ* orientation of Bering Sea euphausiids, so distributions of euphausiid orientations from other studies (Kils, 1981; Endo, 1993; Demer and Conti, 2005; Conti and Demer, 2006) were used to evaluate the effect on DWBA model predictions. Orientation has a large effect on model predictions of euphausiid TS, particularly at higher frequencies (Figure 7). As expected, broadside incidence produced the largest TS values (Figure 7) and distributions with animals swimming nearly horizontally (Demer and Conti, 2005, and Conti and Demer, 2006 orientation distributions) had TS estimates close to measurements made at broadside incidence. Properly characterizing the distribution of orientation for the specific animals and location being studied is clearly important, although these observations are difficult to collect *in situ*.

Numerical density estimates

While there were large differences in euphausiid numerical densities measured acoustically or by net tow, there were also significant differences in euphausiid numerical density depending on what material property values were used in the TS model. Different spatial regions of our study area had euphausiids with significantly different material property values (Smith *et al.*, 2010), and we showed one comparison (DTs 2 and 9) in which using site-specific information (rather than mean values) in the TS modelling revealed the same relative patterns as the net data. Although this is not conclusive, it does suggest that using site-specific information may provide a more accurate representation of spatial patterns or differences in acoustic estimates of zooplankton biomass. It may be difficult to implement for every acoustic survey, but the most accurate numerical density estimates would result from a TS model parameterized with site-specific material and physical animal properties.

We do not fully understand what factors cause the spatial variation in *g* and *h* that have been found previously (Smith *et al.*, 2010) although internal changes in the animal's physiology or composition are logical explanations. Forman and Warren (2010) found that gravid and non-gravid crustaceans (and the eggs) all had different *g* values which may be the result of different levels of energy storage or expenditure by individual animals. Smith *et al.* (2010) showed that *g* values varied with animal size and environmental factors (specifically chlorophyll-a and temperature), which is consistent with the theory that material properties are related to levels of food availability or metabolic requirements of the krill as it uses or stores lipids, or builds muscle or other structures.

The acoustic estimates of euphausiid density in euphausiid layers sampled with trawls were much higher than densities estimated from the catch in the trawls. This is universally true when such comparisons have been made in the literature (e.g. Coyle and Pinchuk, 2002; Warren *et al.*, 2003; Warren and Wiebe, 2008). It is not clear whether the net capture or acoustic estimates more correctly represent the true density of euphausiids at these stations. It is difficult to quantify the uncertainty or possible bias in single net sample estimates (Clutter and Anraku, 1968), but it has been shown experimentally that euphausiids can often avoid capture by nets, leading to 2–20 fold underestimates by net samples (Sameoto *et al.*, 1993; Wiebe *et al.*, 2004). Other explanations for an overestimate of euphausiid density by acoustic techniques could include contributions to Sv from organisms other than euphausiids, or a low bias in model-derived TS predictions.

Methot tows where scattering from age-1 and older walleye pollock occurred in the trawl path were not used for the comparison we presented here, since the MT is not effective at capturing large nekton. Ressler *et al.* (2012) showed that euphausiids often dominated the measured scattering from crustacean mesozooplankton in the Bering Sea, and in some cases our site-specific acoustic estimates of numerical density (e.g. compare estimated densities at DT 2 and 9, Figure 8) were greater than the net data by a factor of approximately 20 or less, which could be entirely due to net avoidance. However, since we cannot rule out contributions to scattering from unretained organisms (Warren and Wiebe, 2008), the acoustic estimates of the numerical density of euphausiids presented here may be overestimated (Warren *et al.*, 2002).

In addition, since the animals used for material properties measurements were collected from different tows than those used for comparison of numerical densities estimated acoustically and via net capture (Table 2), there may be additional uncertainties in comparing net and acoustic estimates due to the horizontal (Smith *et al.*, 2010) or vertical spatial variation in the material properties of euphausiids. Measurement of material properties at depth is difficult and has only successfully been done for *h* (and not *g*) for Southern Ocean euphausiids and copepods (Chu and Wiebe, 2005). Results from their study were mixed with one krill species (*Euphausia superba*) having no variation in *h* with depth, but copepods and a different krill (*E. crystallorophias*) did. Further work on material properties, *in situ* orientation, TS model validation, and comparisons of acoustic estimates of euphausiid density with other techniques are needed to resolve this question. At present, acoustic estimates may best be considered an upper bound (and net capture estimates a lower bound) on the numerical density of euphausiids (Warren and Wiebe, 2008).

Recommendations

Several of the parameters we evaluated have the potential to alter model predictions of euphausiid TS by several orders of magnitude, leading to similar uncertainties in euphausiid population estimates. Since many of these parameters (e.g. length, orientation, material properties) will vary within a typical survey area (and sometimes even within a single aggregation of krill), values used to calculate a mean TS value to produce biomass estimates should be chosen (and tested) carefully. Measurements of the material properties and shape of Bering Sea euphausiids constrained the uncertainty in model TS estimates in this study, but despite the demonstrably improved information on shape and material properties, the disparity between acoustic and net sample estimates of euphausiid densities remained large. Correctly characterizing the *in situ* orientation of euphausiids remains a challenge, and more observations are needed. Our results demonstrate that uncertainty in TS model predictions is reduced if models are parameterized for specific zooplankton taxa in the region of study, rather than applying parameters for other taxa in other regions (commonly done due to a lack of data for many species). Though it presents logistical challenges, acoustic surveys over large areas may need to measure scattering model inputs at multiple sites, particularly in

regions where environmental or zooplankton characteristics may vary greatly.

Acknowledgements

This project was supported by the Alaska Fisheries Science Center, National Marine Fisheries Service, NOAA, and the North Pacific Research Board's Bering Sea Integrated Ecosystem Research Program. The captain, crew, and scientists aboard the NOAA ship *Oscar Dyson* provided excellent logistical support and sampling assistance. Abigail McCarthy helped us greatly with the set up and maintenance of the on board aquaria as well as with the trawl sampling operations. The comments of Dezhang Chu, Kresimir Williams, and several anonymous reviewers helped improve this manuscript. This is NPRB publication number 352 and BEST-BSIERP publication number 64. The findings and conclusions in the paper are those of the authors and do not necessarily represent the views of the National Marine Fisheries Service.

References

Amakasu, K., and Furusawa, M. 2006. The target strength of Antarctic krill (*Euphausia superba*) measured by the split-beam method in a small tank at 70 kHz. ICES Journal of Marine Science, 63: 36–45.

Bailey, K. M. 1989. Interaction between the vertical distribution of juvenile walleye pollock *Theragra chalcogramma* in the eastern Bering Sea, and cannibalism. Marine Ecology Progress Series, 53: 205–213.

Chu, D., Foote, K. G., and Stanton, T. K. 1993. Further analysis of target strength measurements of Antarctic krill at 38 and 120 kHz: Comparison with deformed cylinder model and inference of orientation distribution. Journal of the Acoustical Society of America, 93: 2985–2988.

Chu, D., and Wiebe, P. H. 2005. Measurements of sound-speed and density contrasts of zooplankton in Antarctic waters. ICES Journal of Marine Science, 62: 818–831.

Chu, D., Wiebe, P. H., and Copley, N. 2000. Inference of material properties of zooplankton from acoustic and resistivity measurements. ICES Journal of Marine Science, 57: 1128–1142.

Clutter, R. I., and Anraku, M., 1968. Avoidance of samplers. *In* Zooplankton Sampling UNESCO Monographs in Oceanographic Methodology 2, pp. 57–76. Unesco Press, Paris. 174 pp.

Conti, S. G., and Demer, D. A. 2006. Improved parameterization of the SDWBA for estimating krill target strength. ICES Journal of Marine Science, 63: 928–935.

Coyle, K. O., and Pinchuk, A. I. 2002. The abundance and distribution of euphausiids and zero-age pollock on the inner shelf of the southeast Bering Sea near the Inner Front in 1997-1999. Deep-Sea Research II, 49: 6009–6030.

Decker, M. B., and Hunt, G. L., Jr. 1996. Murre foraging at the frontal system surrounding the Pribilof Islands, Alaska. Marine Ecology Progress Series, 139: 1–10.

Demer, D. A., and Conti, S. G. 2003a. Reconciling theoretical versus empirical target strengths of krill: effects of phase variability on the distorted-wave Born approximation. ICES Journal of Marine Science, 60: 429–434.

Demer, D. A., and Conti, S. G. 2003b. Validation of the stochastic distorted-wave Born approximation model with broad bandwidth total target strength measurements of Antarctic krill. ICES Journal of Marine Science, 60: 625–635.

Demer, D. A., and Conti, S. G. 2005. New target-strength model indicates more krill in the Southern Ocean. ICES Journal of Marine Science, 62: 25–32.

De Robertis, A., McKelvey, D. R., and Ressler, P. H. 2010. Development and application of an empirical multifrequency method for backscatter classification. Canadian Journal of Fisheries and Aquatic Sciences, 67 : 1459–1474.

Endo, Y. 1993. Orientation of Antarctic krill in an aquarium. Nippon Suisan Gakkaishi, 59: 465–468.

FAO. 2009. The State of World Fisheries and Aquaculture 2008, Part 1. World Review of Fisheries and Aquaculture. FAO Fisheries and Aquaculture Department. 176 pp. http://www.fao.org/docrep/011/i0250e/i0250e00.htm (last accessed 28 July 2012).

Foote, K. G. 1990. Speed of sound in Euphausia superba. Journal of the Acoustical Society of America, 87: 1405–1408.

Foote, K. G., Knudsen, H. P., Vestnes, G., MacLennan, D. N., and Simmonds, E. J. 1987. Calibration of acoustic instruments for fish density estimates: a practical guide. ICES Cooperative Research Report 144. 69 pp.

Foote, K. G., and Stanton, T. K. 2000. Acoustical methods. In ICES Zooplankton Methodology Manual, pp. 223–258. Ed. by R. Harris, P. Wiebe, J. Lenz, H. Skjoldal, and M. Huntley. Academic Press, London.

Forman, K. A., and Warren, J. D. 2010. Variability in the density and sound-speed of coastal zooplankton and nekton. ICES Journal of Marine Science, 67, 10–18. doi:10.1093/icesjms/fsp217.

Gorska, N., Ona, E., and Korneliussen, R. 2005. Acoustic backscattering by Atlantic mackerel as being representative of fish that lack a swimbladder. Backscattering by individual fish. ICES Journal of Marine Science, 62: 984–995.

Greenlaw, C. F., and Johnson, R. K. 1982. Physical and acoustical properties of zooplankton. Journal of the Acoustical Society of America, 72: 1706–1710.

Hatch, S. A., and Sanger, G. A. 1992. Puffins as samplers of juvenile pollock and other forage fish in the Gulf of Alaska. Marine Ecology Progress Series, 80: 1–14.

Honkalehto, T., Jones, D., McCarthy, A., McKelvey, D., Guttormsen, M., Williams, K., and Williamson, N. 2009. Results of the Echo Integration-Trawl Survey of Walleye Pollock (*Theragra chalcogramma*) on the U.S. and Russian Bering Sea Shelf in June and July 2008. NOAA Technical Memorandum NMFS-AFSC-194, 56 pp. http://www.afsc.noaa.gov/Publications/AFSC-TM/NOAA-TM-AFSC-194.pdf (last accessed 28 July 2012).

Ianelli, J. N., Barbeaux, S., Honkalehto, T., Kotwicki, S., Aydin, K., and Williamson, N. 2009. Assessment of the walleye pollock stock in the Eastern Bering Sea, p. 47–136.*In* Stock Assessment. NPFMC Bering Sea and Aleutian Islands Stock Assessment and Fishery Evaluation (SAFE) Document 605W.

Jones, B. A., Lavery, A. C., and Stanton, T. K. 2009. Use of the distorted wave Born approximation to predict scattering by inhomogeneous objects: Applications to squid. Journal of the Acoustical Society of America, 125: 73–88.

Kasatkina, S. M., Gross, C., Emery, J. H., Takao, Y., Litvinov, F. F., Malyshko, A., Shnar, V. N., *et al.* 2004. A comparison of net and acoustic estimates of krill density in the Scotia Sea during the CCAMLR 2000 Survey. Deep-Sea Research II, 51: 1289–1300.

Kils, U. 1981. Swimming Behavior, Swimming Performance and Energy Balance of Antarctic Krill, Euphausia superba. BIOMASS Science Series 3.

Køgeler, J. W., Falk-Petersen, S., Kristensen, Å., Pettersen, F., and Dalen, J. 1987. Density- and sound speed contrasts in sub-Arctic zooplankton. Polar Biology, 7: 231–235.

Kristensen, A., and Dalen, J. 1986. Acoustic estimation of size distribution and abundance ofzooplankton. Journal of the Acoustical Society of America, 80: 601–611.

Lang, G. M., Brodeur, R. D., Napp, J. M., and Schabetsberger, R. 2000. Variation in groundfish predation on juvenile walleye pollock relative to hydrographic structure near the Pribilof Islands, Alaska. ICES Journal of Marine Science, 57: 265–271.

Lang, G. M., Livingston, P. A., and Dodd, K. A. 2005. Groundfish Food Habits and Predation on Commercially Important Prey Species in the Eastern Bering Sea from 1997 Through 2001. NOAA Technical Memorandum NMFS-AFSC-158. 230pp.

Lavery, A. C., Stanton, T. K., McGehee, D. E., and Chu, D. 2002. Three-dimensional modelling of acoustic backscattering from fluid-like zooplankton. Journal of the Acoustical Society of America, 111: 1197–1210.

Lawson, G. L., Wiebe, P. H., Ashjian, C. J., Chu, D., and Stanton, T. K. 2006. Improved parameterization of Antarctic krill target strength models. Journal of the Acoustical Society of America, 119: 232–242.

Lawson, G. L., Wiebe, P. H., Stanton, T. K., and Ashjian, C. J. 2008. Euphausiid distribution along the Western Antarctic Peninsula-Part A: Development of robust multi-frequency acoustic techniques to identify euphausiid aggregates and quantify euphausiid size, abundance, and biomass. Deep-Sea Research. Part 2. Topical Studies in Oceanography, 55: 412–431.

Lee, K., Mukai, T., Lee, D., and Iida, K. 2008. Verification of mean volume backscattering strength obtained from acoustic Doppler current profiler by using sound scattering layer. Fisheries Science, 74: 221–229.

McGehee, D. E., O'Driscoll, R. L., and Martin-Traykovski, L. V. 1998. Effects of orientation on acoustic scattering from Antarctic krill at 120 kHz. Deep Sea Research II, 45: 1273–1294.

Medwin, H., and Clay, C. S. 1998. Fundamentals of Acoustical Oceanography. Academic Press, San Diego, California.

Methot, R. D. 1986. Frame trawl for sampling pelagic juvenile fish. CalCOFI Reports, 27: 267–278.

Miyashita, K. 2003. Diurnal changes in the acoustic-frequency characteristics of Japanese anchovy (*Eugraulis japonicus*) post-larvae "shirasu" inferred from theoretical scattering models. ICES Journal of Marine Science, 60: 532–537.

Morse, P. M., and Ingard, K. U. 1968. Theoretical Acoustics. Princeton University Press, Princeton, NJ.

Reiss, C. S., Cossio, A. M., Loeb, V., and Demer, D. A. 2008. Variations in the biomass of Antarctic krill (*Euphausia superba*) around the South Shetland Islands, 1996-2006. ICES Journal of Marine Science, 65: 497–508.

Ressler, P. H., De Robertis, A., Warren, J. D., Smith, J. N., and Kotwicki, S. 2012. Developing an acoustic index of euphausiid abundance to understand trophic interactions in the Bering Sea ecosystem. Deep-Sea Research II, 65–70: 184–195.

Sameoto, D., Cochrane, N., and Herman, A. 1993. Convergence of acoustic, optical, and net-catch estimates of euphausiid abundance: Use of artificial light to reduce net avoidance. Canadian Journal of Fisheries and Aquatic Sciences, 50: 334–346.

Simmonds, J., and MacLennan, D. 2005. Fisheries Acoustics: Theory and Practice, 2nd edn. Blackwell Science Ltd., Oxford, UK. 437 pp.

Sinclair, E. 1994. Prey selection by northern fur seals (*Callorhinus ursinus*) in the eastern Bering Sea. Fisheries Bulletin, 92: 144–156.

Smith, J. N., Ressler, P. H., and Warren, J. D. 2010. Material properties of euphausiids and other zooplankton from the Bering Sea. Journal of the Acoustical Society of America, 128: 2664–2680.

Stanton, T. K. 1988a. Sound scattering by cylinders of finite length I: Fluid cylinders. Journal of the Acoustical Society of America, 83: 55–63.

Stanton, T. K. 1988b. Sound scattering by cylinders of finite length II. Elastic cylinders. Journal of the Acoustical Society of America, 83: 64–67.

Stanton, T. K. 1989. Sound scattering by cylinders of finite length III: Deformed cylinders. Journal of the Acoustical Society of America, 86: 691–705.

Stanton, T. K., Chu, D., Wiebe, P. H., and Clay, C. S. 1993a. Average echoes from randomly oriented random-length finite cylinders: Zooplankton models. Journal of the Acoustical Society of America, 96: 3463–3472.

Stanton, T. K., Clay, C. S., and Chu, D. 1993b. Ray representation of sound scattering by weakly scattering deformed fluid cylinders: Simple physics and application to zooplankton. Journal of the Acoustical Society of America, 94: 3454–3462.

Stanton, T. K., and Chu, D. 2000. Review and recommendations for the modelling of acoustic scattering by fluid-like elongated zooplankton: euphausiids and copepods. ICES Journal of Marine Science, 57: 793–807.

Stanton, T. K., Chu, D, and Wiebe, P. H. 1998a. Sound scattering by several zooplankton groups. II. Scattering models. Journal of the Acoustical Society of America, 103: 236–253.

Stanton, T. K., Wiebe, P. H., and Chu, D. 1998b. Differences between sound scattering by weakly scattering spheres and finite-length cylinders with applications to sound scattering by zooplankton. Journal of the Acoustical Society of America, 103: 254–264.

Urick, R. J. 1983. Principles of Underwater Sound, 3rd edn. McGraw-Hill, Inc. Peninsula Publishing, Los Altos, California.

Warren, J. D., Stanton, T. K, McGehee, D. E., and Chu, D. 2002. Effect of animal orientation on acoustic estimates of zooplankton properties. IEEE Journal of Oceanic Engineering, 27: 130–138.

Warren, J. D., Stanton, T. K., Wiebe, P. H., and Seim, H. E. 2003. Inference of biological and physical parameters in an internal wave using multiple frequency acoustic scattering data. ICES Journal of Marine Science, 60: 1033–1046.

Warren, J. D., and Wiebe, P. H. 2008. Accounting for biological and physical sources of acoustic scattering improves estimates of zooplankton biomass. Canadian Journal of Fisheries and Aquatic Sciences, 65: 1321–1333. doi:10.1139/F08-047.

Wiebe, P. H., Ashjian, C. J., Gallager, S. M., Davis, C. S., Lawson, G. L., and Copley, N. J. 2004. Using a high-powered strobe light to increase the catch of Antarctic krill. Marine Biology, 144: 493–502.

Wiebe, P. H., Chu, D., Kaartvedt, S., Hundt, A., Melle, W., Ona, E., and Batta-Lona, P. 2010. The acoustic properties of *Salpa thompsoni*. ICES Journal of Marine Science, 67: 583–593.

Handling editor: Stéphane Plourde